Food Chemistry 179 (2015) 6–14

Contents lists available at ScienceDirect

Food Chemistry

journal homepage: www.elsevier.com/locate/foodchem

Edible flowers of *Viola tricolor* L. as a new functional food: Antioxidant activity, individual phenolics and effects of gamma and electron-beam irradiation

Amanda Koike [a,b], João C.M. Barreira [a,c], Lillian Barros [a], Celestino Santos-Buelga [c], Anna L.C.H. Villavicencio [b], Isabel C.F.R. Ferreira [a,*]

[a] Mountain Research Centre (CIMO), ESA, Polytechnic Institute of Bragança, Campus de Santa Apolónia, Ap. 1172, 5301-855 Bragança, Portugal
[b] Nuclear and Energy Research Institute, National Commission of Nuclear Energy – IPEN/CNEN-SP, Av. Professor Lineu Prestes 2242, Butantã 05508-000, São Paulo, Brazil
[c] Grupo de Investigación en Polifenoles (GIP-USAL), Faculty of Pharmacy, University of Salamanca, Campus Miguel de Unamuno, 37007 Salamanca, Spain

ARTICLE INFO

Article history:
Received 29 October 2014
Received in revised form 22 December 2014
Accepted 27 January 2015
Available online 31 January 2015

Keywords:
Viola tricolor
HPLC–DAD–ESI/MS
Phenolic compounds
Antioxidant activity
Linear discriminant analysis

ABSTRACT

Edible flowers are used in food preparations, being also recognized for their beneficial effects on human health. Nevertheless, these species are highly perishable, and irradiation treatment might be applied to ensure food quality and increase their shelf life. *Viola tricolor* L. is a typical edible flower, with multiple applications and biological properties, mainly provided by the flavonoid content. In the present work, the phenolic compounds were analyzed by HPLC–DAD–ESI/MS, and the antioxidant activity was evaluated using biochemical assays. Linear discriminant analyses (LDA) were performed in order to compare the results obtained with flowers submitted to different irradiation doses and technologies (cobalt-60 and electron-beam). In general, irradiated samples (mostly with 1 kGy) showed the highest phenolic content and antioxidant activity. Furthermore, the significant differences observed in the LDA allow determination of which dose and/or technology is suitable to obtain flowers with higher antioxidant potential.

1. Introduction

Edible flowers have been used in culinary preparations to improve the sensorial and nutritional qualities of food, by adding color, flavor, taste and visual appeal to culinary preparations. They are used in sauces, jellies, syrups, liquors, vinegars, honey, oils, candied flowers, ice cubes, salads, teas and other beverages, and different desserts. Furthermore, edible flowers are important for human health due to their richness in bioactive and nutraceutical compounds, which offers additional marketing opportunities (Creasy, 1999; Mlcek & Rop, 2011; Anderson, Schnelle, & Bastin, 2012).

Nevertheless, edible flowers are highly perishable and must be free of insects, which is difficult because these flowers are usually cultivated without using any pesticide. Their high perishability requires storage in small plastic packages under refrigerated environments, which poses an additional cost in the commercial chain (Kelley, Cameron, Biernbaum, & Poff, 2003; Newman & O'Conner, 2009).

Several methods are used by the food industry to increase the shelf life of food products, but also to ensure their quality and safety, which is important to guarantee the public health (Farkas & Mohácsi-Farkas, 2011). Food irradiation is an economically viable technology to extend shelf life of perishable commodities, improving their hygiene and quality, but also allowing the disinfestation of insects (Fan, Niemira, & Sokorai, 2003). Radiation processing (the use of ionizing radiations from isotopes of cobalt or from electron-accelerators) has been used in several countries, and its efficiency and safety has been approved by authorities, namely the FDA, USDA, WHO, FAO, and also by scientific societies based on extensive research (Morehouse, 2002; Farkas, 2006; Komolprasert, 2007).

Viola tricolor L. (heartseases), from *Violaceae* family, represents one of the most popular sources of edible flowers. Disseminated through Europe and Asia, the flowers are small and delicate, with blue, yellow, purple, pink or white color, and sometimes, combined colors in the same flower (Mlcek & Rop, 2011; Jauron, Beiwel, & Naeve, 2013). *V. tricolor* has a refreshing taste and velvety texture which allow its use in sweets, salads, soups, vinegars, drinks, and also in the extraction of blue and yellow food colourings (Creasy, 1999; Newman & O'Conner, 2009). Heartsease flowers, apart from being used as food, have also been used as medicinal agents for thousands of years. Their biological activities (Hellinger et al., 2014), mainly antioxidant properties, are attributed to the

* Corresponding author. Tel.: +351 273 303219; fax: +351 273 325405.
E-mail address: iferreira@ipb.pt (I.C.F.R. Ferreira).

http://dx.doi.org/10.1016/j.foodchem.2015.01.123
0308-8146/

presence of flavonoid compounds (Vukics, Kery, Bonn, & Guttman, 2008; Vukics, Ringer, Kery, Bonn, & Guttman, 2008; Piana et al., 2013), with violanthin reported as the major compound (Vukics, Kery, et al., 2008).

The purpose of this study was to characterize the phenolic profile and the antioxidant activity of *V. tricolor* flowers of Brazilian origin, and to evaluate the effects of different electron-beam and gamma irradiation doses on these two bioactive indicators (*i.e.*, phenolic compounds and antioxidant activity).

2. Materials and methods

2.1. Samples

Fresh flowers of *V. tricolor* were purchased from a local market in São Paulo, Brazil, in November 2013. Heartsease petals with different phenotypes (yellow, orange, purple, white and multicolored) were pooled together prior to laboratory analyses.

2.2. Samples irradiation

2.2.1. Gamma irradiation

The samples were irradiated at the Nuclear and Energy Research Institute – IPEN/CNEN (São Paulo, Brazil), using a ^{60}Co source Gammacell 200 (Nordion Ltd., Ottawa, ON, Canada), at room temperature, with a dose rate of 1.230 kGy/h, at doses of 0.5, 0.8 and 1 kGy. Harwell Amber 3042 dosimeters were used to measure the radiation dose. Non-irradiated samples were used as control. After irradiation, the samples were lyophilized (Solab SL404, São Paulo, Brazil), powdered and stored inside polyethylene bags kept in a desiccator at room temperature for subsequent use.

2.2.2. Electron-beam irradiation

Samples were irradiated at the Nuclear and Energy Research Institute – IPEN/CNEN (São Paulo, Brazil), using an electron-beam accelerator (Dynamitron, Radiation Dynamics Inc., Edgewood, NY, USA), at room temperature. The applied doses were 0.5 kGy (dose rate: 1.11 kGy/s, energy: 1.400 MeV, beam current: 0.3 mA, tray speed: 6.72 m/min), 0.8 kGy (dose rate: 1.78 kGy/s, energy: 1.400 MeV, beam current: 0.48 mA, tray speed: 6.72 m/min) and 1 kGy (dose rate: 2.23 kGy/s, energy: 1.400 MeV, beam current: 0.6 mA, tray speed: 6.72 m/min). Non-irradiated samples were used as a control. After irradiation, the samples were lyophilized (Solab SL404, São Paulo, Brazil), powdered and stored inside polyethylene bags, and kept in a desiccator at room temperature for subsequent use.

2.3. Analysis of phenolic compounds

2.3.1. Analysis of non-anthocyanin phenolic compounds

The samples (≈0.5 g) were extracted by stirring with 20 ml of methanol/water 80:20 (*v*/*v*), at room temperature, 150 rpm, for 1 h. The extract was filtered through Whatman No. 4 paper. The residue was then re-extracted with additional portions (20 ml) of methanol/water 80:20 (*v*/*v*). The combined extracts were then evaporated at 35 °C (rotary evaporator Büchi R-210, Flawil, Switzerland) to remove methanol. The aqueous phase was lyophilized, and 10 mg were re-dissolved in 2 ml of 20% aqueous methanol and filtered through a 0.22-μm disposable LC filter disk for high performance liquid chromatography (HPLC–DAD–MS) analysis. The extracts were analyzed using a Hewlett–Packard 1100 chromatograph (Agilent Technologies, Santa Clara, CA, USA) with a quaternary pump and a diode array detector (DAD) coupled to an HP Chem Station (rev. A.05.04) data-processing station. A Waters Spherisorb S3 ODS-2 C_{18}, 3 μm (4.6 mm × 150 mm) column thermostatted at 35 °C was used. The solvents used were: (A) 0.1% formic acid in water, (B) acetonitrile. The elution gradient established was 10% B to 15% B over 5 min, 15–25% B over 5 min, 25–35% B over 10 min, isocratic 50% B for 10 min, and re-equilibration of the column, using a flow rate of 0.5 ml/min. Double online detection was carried out in the DAD using 280 nm and 370 nm as preferred wavelengths, and in a mass spectrometer (MS) connected to the HPLC system via the DAD cell outlet.

MS detection was performed in an API 3200 Qtrap (Applied Biosystems, Darmstadt, Germany) equipped with an ESI source and a triple quadrupole-ion trap mass analyzer that was controlled by Analyst 5.1 software. Zero grade air served as the nebulizer gas (30 psi) and turbo gas for solvent drying (400 °C, 40 psi). Nitrogen served as the curtain (20 psi) and collision gas (medium). The quadrupoles were set at unit resolution. The ion spray voltage was set at −4500 V in the negative mode. The MS detector was programmed to perform a series of two consecutive modes: enhanced MS (EMS) and enhanced product ion (EPI) analysis. EMS was employed to record full scan spectra in order to obtain an overview of all of the ions in the sample. The settings used were: declustering potential (DP) −450 V, entrance potential (EP) −6 V, and collision energy (CE) −10 V. Spectra were recorded in negative ion mode between *m*/*z* 100 and 1500. Analysis in EPI mode was further performed in order to obtain the fragmentation pattern of the parent ion(s) detected in the previous experiment using the following parameters: DP −50 V, EP −6 V, CE −25 V, and collision energy spread (CES) 0 V.

The phenolic compounds present in the samples were characterized according to their UV and mass spectra, and retention times compared with commercial standards when available. Otherwise, peaks were tentatively identified by comparing the obtained information with available data reported in the literature. For the quantitative analysis of phenolic compounds, a calibration curve was obtained by injection of known concentrations (1–100 μg/ml) of different standard compounds: isorhamnetin-3-*O*-rutinoside ($y = 258.42x + 10.647$; $R^2 = 0.999$), quercetin-3-*O*-rutinoside ($y = 222.79x + 243.11$; $R^2 = 1.000$), kaempferol-3-*O*-rutinoside ($y = 175.02x - 43.887$; $R^2 = 1.000$) and apigenin-6-*C*-glucoside ($y = 246.05x - 309.66$). Quantification was performed based on DAD results from the areas of the peaks recorded at 280 nm or 370 nm, and results were expressed in mg/g of extract.

2.3.2. Analysis of anthocyanins

Each sample (≈0.5 g) was extracted with 20 ml of methanol containing 0.5% trifluoroacetic acid (TFA), and filtered through a Whatman n° 4 paper. The residue was then re-extracted with additional 20 ml portions of 0.5% TFA in methanol. The combined extracts were evaporated at 35 °C to remove the methanol, and re-dissolved in water. For purification, the extract solution was deposited onto a C-18 SepPak® Vac 3 cc cartridge (Phenomenex, Torrance, CA, USA), previously activated with methanol followed by water. Sugars and more polar substances were removed by passing through 10 ml of water, and anthocyanin pigments were further eluted with 5 ml of methanol/water (80:20, *v*/*v*) containing 0.1% TFA. The extract was concentrated under vacuum, lyophilized, re-dissolved in 1 ml of 20% aqueous methanol and filtered through a 0.22-μm disposable LC filter disk for HPLC analysis.

The extracts were analyzed in the HPLC system indicated above using previously described conditions (García-Marino, Hernández-Hierro, Rivas-Gonzalo, & Escribano-Bailón, 2010). Separation was achieved on an AQUA®(Phenomenex, Torrance, CA, USA) reverse phase C_{18} column (5 μm, 150 mm × 4.6 mm i.d) thermostatted at 35 °C. The solvents used were: (A) 0.1% TFA in water, and (B) 100% acetonitrile. The gradient employed was: isocratic 10% B for 3 min, from 10% to 15% B for 12 min, isocratic 15% B for 5 min, from

15% to 18% B for 5 min, from 18% to 30% B for 20 min and from 30% to 35% B for 5 min, at a flow rate of 0.5 ml/min. Double detection was carried out by DAD, using 520 nm as the preferred wavelength, and MS using the same equipment described above. Zero grade air served as the nebulizer gas (40 psi) and turbo gas (600 °C) for solvent drying (50 psi). Nitrogen served as the curtain (100 psi) and collision gas (high). Both quadrupoles were set at unit resolution. The ion spray voltage was set at 5000 V in the positive ion mode. EMS and ESI methods were used for acquisition of full scan spectra and fragmentation patterns of the precursor ions, respectively. Setting parameters used for EMS mode were: declustering potential (DP) 41 V, entrance potential (EP) 7.5 V, collision energy (CE) 10 V, and parameters for EPI mode were: DP 41 V, EP 7.5 V, CE 10 V, and collision energy spread (CES) 0 V.

The anthocyanins present in the samples were characterized according to their UV/mass spectra and retention times, and comparison made with available standards. For quantitative analysis, a calibration curve was obtained by injection of known concentrations (50–0.25 μg/ml) of delphinidin-3-*O*-glucoside ($y = 557274x + 126.24$; $R^2 = 0.9997$) and cyanidin-3-*O*-glucoside ($y = 630276x - 153.83$; $R^2 = 0.9995$). Quantification was performed based on DAD results from the areas of the peaks recorded at 520 nm, and results were expressed in μg/g of extract.

2.4. Evaluation of antioxidant activity

2.4.1. General

The methanol/water extract described above (Section 2.3.1) was used in the antioxidant activity assays. Successive dilutions were prepared from a stock solution of 20 mg/ml and submitted to *in vitro* antioxidant activity assays. The sample concentrations (mg/ml) providing 50% of antioxidant activity or 0.5 of absorbance (EC_{50}) were calculated from the graphs of antioxidant activity percentages (DPPH and β-carotene/linoleate assays) or absorbance at 690 nm (Prussian blue assay), respectively. Trolox was used as a positive control.

2.4.2. DPPH radical-scavenging activity

The reaction mixture consisted of different concentrations (30 μL) of the extract solutions and methanolic solution (270 μL) containing DPPH radicals (6×10^{-5} mol/L) in different wells of a 96 well microplate. The mixture was left to stand in the dark for 30 min, and the absorbance was measured at 515 nm (microplate reader mentioned above). The radical scavenging activity (RSA) was calculated as the percentage of DPPH discoloration: $\%RSA = [(A_{DPPH} - A_S)/A_{DPPH}] \times 100$, where A_S is the absorbance of the solution containing the sample, and A_{DPPH} is the absorbance of the DPPH solution.

2.4.3. Reducing power

Two different procedures were used to evaluate the reducing power:

The first methodology followed the Prussian blue assay and was performed using a Microplate Reader EL×800 Microplate Reader (Bio-Tek Instruments, Inc., Winooski, VT, USA). The different concentrations of the extracts (0.5 ml) were mixed with sodium phosphate buffer (200 mmol L^{-1}, pH 6.6, 0.5 ml) and potassium ferricyanide (1% *w*/*v*, 0.5 ml). For each concentration, the mixture was incubated at 50 °C for 20 min, and trichloroacetic acid (10% *w*/*v*, 0.5 ml) was added. The mixture (0.8 ml) was poured into the 48-wells, along with deionized water (0.8 ml) and ferric chloride (0.1% *w*/*v*, 0.16 ml), and the absorbance was measured at 690 nm.

The second methodology followed the Folin–Ciocalteu assay. The extract solution (1 ml) was mixed with Folin–Ciocalteu reagent (5 ml, previously diluted with water 1:10, *v*/*v*) and sodium carbonate (75 g/L, 4 ml). The tubes were vortex mixed for 15 s and allowed to stand for 30 min at 40 °C for color development. The absorbance was then measured at 765 nm. Gallic acid was used to calculate the standard curve and the results were expressed as mg of gallic acid equivalents (GAE) per g of extract.

2.4.4. Inhibition of β-carotene bleaching or β-carotene/linoleate assay

A solution of β-carotene was prepared by dissolving β-carotene (2 mg) in chloroform (10 ml). 2 ml of this solution were pipetted

Table 1
Retention time (Rt), wavelengths of maximum absorption (λ_{max}), mass spectral data, relative abundances of fragment ions and tentative identification of the phenolic compounds in *Viola tricolor* extracts.

Compound	R_t (min)	λ_{max} (nm)	Molecular ion (*m*/*z*)	MS^2 (*m*/*z*)	Tentative identification
1	14.3	228, 260, 306sh, 358	771	315(100)	Isorhamnetin-hexosyl-pentosyl-hexoside
2	15.2	256, 266sh, 300sh, 356	755	609(2), 591(3), 489(4), 343(2), 301(100)	Quercetin-3-*O*-(6-*O*-rhamnosylglucoside)-7-*O*-rhamnoside
3	15.5	232, 266, 306sh, 350	623	315(100)	Isorhamnetin-3-*O*-(6-*O*-rhamosyl-galactoside)
4	15.7	256, 266sh, 298sh, 354	797	755(20), 489(3), 301(100)	Acetyl-quercetin-3-*O*-(6-*O*-rhamnosylglucoside)-7-*O*-rhamnoside
5	16.1	266, 300sh, 348	739	593(3), 285(100)	Kaempferol-3-*O*-(6-*O*-rhamnosylglucoside)-7-*O*-rhamnoside
6	16.4	258sh, 272, 346	577	517(2), 487(15), 473(30), 457(27), 383(24), 353(33)	Violanthin (apigenin-6-*C*-glucosyl-8-*C*-rhamnoside)
7	16.6	254, 266sh, 302sh, 354	769	623(12), 605(12), 503(8), 357(8), 315(100)	Isorhamnetin-3-*O*-(2,6-di-*O*-rhamosyl-glucoside)
8	16.9	258, 266sh, 300sh, 354	609	301(100)	Quercetin-3-*O*-rutinoside
9	18.5	266, 300sh, 348	593	285(100)	Kaempferol-3-*O*-rutinoside
10	18.9	254, 266sh, 302sh, 354	623	315(100)	Isorhamnetin-3-*O*-rutinoside
11	18.1	282, 520	595	449(11), 287(100)	Cyanidin-3-*O*-rutinoside
12	26.7	282, 524	611	465(15), 303(100)	Delphinidin-3-*O*-rutinoside
13	28.1	280, 310sh, 530	919	757(26), 465(12), 303(100)	Delphinidin-3-(4″-*p*-coumaroyl)-rutinoside-5-glucoside
14	31.5	282, 312sh, 522	903	741(36), 449(12), 287(100)	Cyanidin-3-(coumaroyl)-methylpentosyl-hexosyl-5-hexoside

into a round-bottom flask. The chloroform was removed at 40 °C under vacuum. Linoleic acid (40 mg), Tween 80 emulsifier (400 mg), and distilled water (100 ml) were added to the flask with vigorous shaking. Aliquots (4.8 ml) of this emulsion were transferred into test tubes containing fraction/extract solutions with different concentrations (0.2 ml). The tubes were shaken and incubated at 50 °C in a water bath. As soon as the emulsion was added to each tube, the zero time absorbance was measured at 470 nm (Analytik 200–2004 spectrophotometer, Jena, Germany). β-Carotene bleaching inhibition was calculated using the following equation: (absorbance after 2 h of assay/initial absorbance) × 100.

2.5. Statistical analysis

Three independent extractions were performed, and each of these replicates was assayed three times. An analysis of variance (ANOVA) with type III sums of squares was performed using the GLM (General Linear Model) procedure of the SPSS software. The fulfilment of the one-way ANOVA requirements, specifically the normal distribution of the residuals and the homogeneity of variance, was tested by means of the Shapiro–Wilk's, and the Levene's tests, respectively. The dependent variables were analyzed using 2-way ANOVA, with the factors "irradiation dose" (ID) and

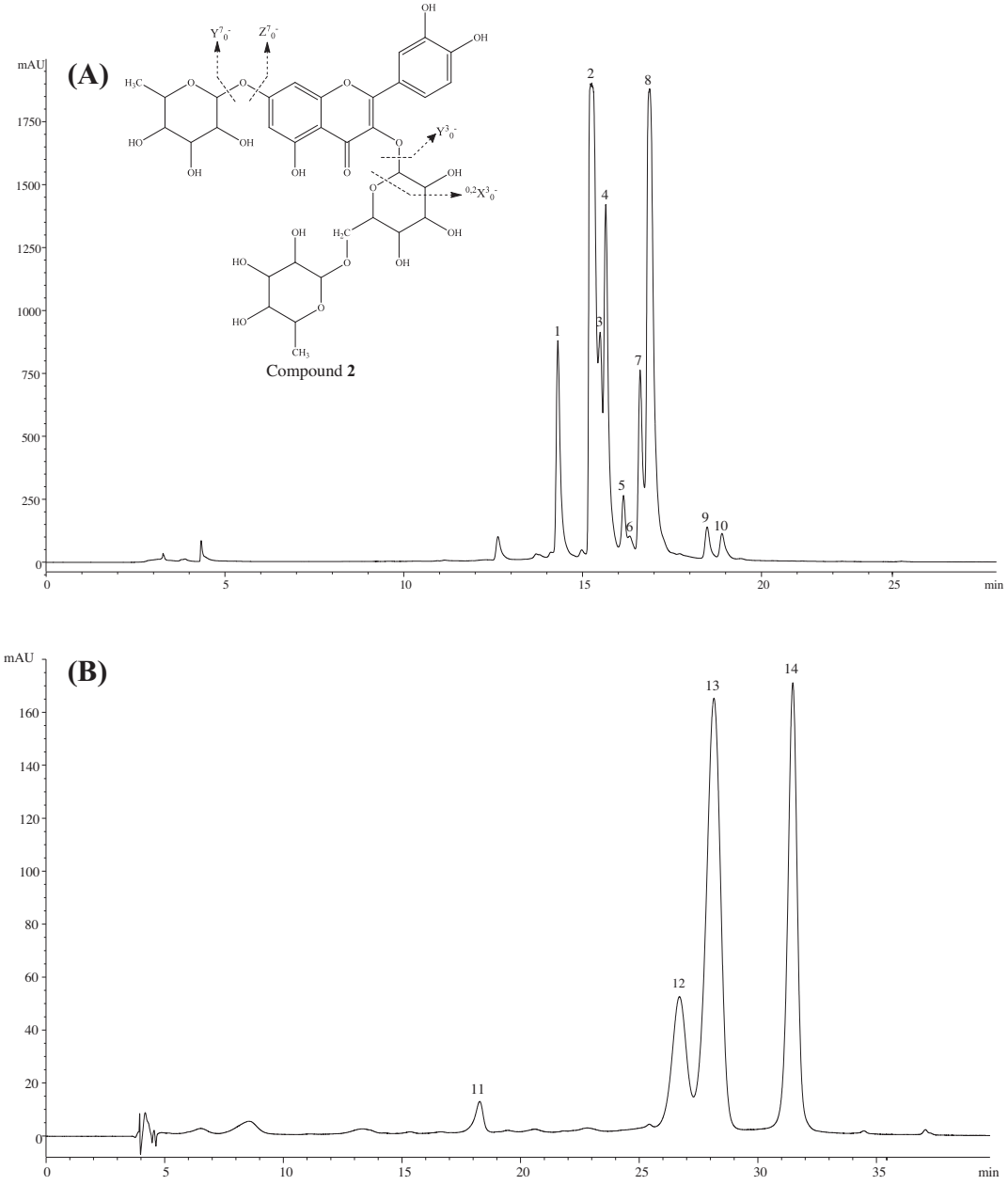

Fig. 1. (A). HPLC chromatogram of the non-anthocyanin phenolic compounds from non-irradiated samples of *Viola tricolor* recorded at 370 nm. **1**: Isorhamnetin-hexosyl-pentosyl-hexoside; **2**: quercetin-3-*O*-deoxyhexosylhexoside-7-*O*-hexoside; **3**: isorhamnetin-3-*O*-(6-*O*-rhamosyl-galactoside); **4**: quercetin-3-*O*-deoxyhexosylhexoside-7-*O*-acetyl-hexoside; **5**: kaempferol-*O*-(di-deoxyhexosyl-hexoside); **6**: violanthin (apigenin-6-*C*-rhamnosyl-8-*C*-glucoside); **7**: isorhamnetin-3-*O*-(2,6-di-*O*-rhamosyl-glucoside); **8**: quercetin-3-*O*-rutinoside; **9**: kaempferol-3-*O*-rutinoside; **10**: isorhamnetin-3-*O*-rutinoside. The suggested structure for compound **2** is depicted with the proposed fragmentation. (B). HPLC chromatogram of the anthocyanins from unirradiated samples of *Viola tricolor* recorded at 370 nm. **11**: Cyanidin-*O*-deoxyhexosyl-hexoside; **12**: delphinidin-*O*-deoxyhexosyl-hexoside; **13**: delphinidin-*O*-di-(deoxyhexosyl-hexoside); **14**: cyanidin-*O*-di-(deoxyhexosyl-hexoside).

"irradiation technology" (IT). When a statistically significant interaction (ID × IT) was detected, the two factors were simultaneously evaluated by the estimated marginal mean plots for all levels of each single factor. Alternatively, if no statistical significant interaction was verified, means were compared using multiple comparison tests, adequate for homoscedastic or heteroscedastic distributions. Results regarding the comparison of electron-beam and gamma irradiation were classified using a simple *t*-test, since there were less than three groups.

In order to obtain a comprehensive interpretation of the results, linear discriminant analysis (LDA) was used to compare the effect of IT and ID on antioxidant activity and phenolic compounds. A stepwise technique, using the Wilks' λ method, with the usual probabilities of F (3.84 to enter and 2.71 to remove), was applied for variable selection. This procedure uses a combination of forward selection and backward elimination processes, in which the inclusion of a new variable comes after ensuring that all variables previously selected remain significant. With this approach, it is possible to identify the significant variables obtained for each factor. To verify the significance of canonical discriminant functions, the Wilks' λ test was applied. A leaving-one-out cross-validation procedure was carried out to assess the model performance.

3. Results and discussion

3.1. Individual phenolic compounds

As previously stated, the bioactivity of edible flowers is highly correlated to phenolic compound composition (Vukics, Kery, et al., 2008; Vukics, Ringer, et al., 2008; Piana et al., 2013). Accordingly, the phenolic profile of *V. tricolor* was characterized by HPLC–DAD–ESI/MS analysis. Data for the retention time, λ_{max}, deprotonated molecule, main fragment ions in MS^2 and tentative identification of the compounds are presented in Table 1. As an example, the HPLC phenolic profile of the control sample (non-irradiated), recorded at 370 nm, is presented in Fig. 1A and B.

UV and mass spectra indicated that the phenolic composition of the analyzed flowers was characterized by the presence of flavonoids, particularly flavone (compound **6**, an apigenin derivative), flavonol (isorhamnetin, quercetin and kaempferol derivatives) and anthocyanin (delphinidin and cyanidin derivatives) classes. The analysis of the MS^2 fragments suggested that, except the apigenin derivative (that was *C*-glycosylated), all the remaining compounds were present as *O*-glycosides. Glycoside substituents consisted of pentosyl, deoxyhexosyl, hexosyl, dideoxyhexosyl, deoxyhexosyl-hexosyl and dihexosyl units, as deduced from the losses of 132, 146, 162, 292, 308 and 324 mu. The presence of flavonoid glycosides was previously reported in German (Hörhammer, Wagner, Rosprim, Mabry, & Rösler, 1965; Wagner, Rosprim, & Düll, 1972), Hungarian (Vukics, Kery, et al., 2008; Vukics, Ringer, et al., 2008) and Brazilian (Gonçalves et al., 2012) samples of *V. tricolor*.

The flavonol glycosides (compounds **1**–**5** and **7**–**10**) show UV spectra typical of flavonol-3-*O*-glycosyl derivatives (Mabry, Markham, & Thomas, 1970) (Table 1). In their MS fragmentation profiles, product ions at m/z 285, 301 or 315 were observed in high abundance, which might correspond to the deprotonated aglycon ions of kaempferol, quercetin and isorhamnetin, respectively.

Fragmentation of compounds **1** ($[M-H]^-$ at m/z 771), **3** ($[M-H]^-$ at m/z 623), **7** ($[M-H]^-$ at m/z 769) and **10** ($[M-H]^-$ at m/z 623), showed the same base peak at m/z 315 coherent with isorhamnetin derivatives, which was also supported by their UV spectra. In compounds **1**, **3** and **10**, only the fragment ion corresponding to the aglycon was produced, suggesting that the sugar moieties were attached to the same position of the flavonoid

Table 2
Quantification (mg/g of dried plant, for compounds **1–10**; μg/g of dried plant, for compounds **11–14**) of the phenolic compounds in *Viola tricolor* extracts according to the irradiation dose (ID) and irradiation technology (IT).

Compound	Tentative identification	Quantification (mg/g of extract)								
		Irradiation dose (ID)				*p*-Value ($n = 18$)	Irradiation technology (IT)		*p*-Value ($n = 36$)	ID × IT *p*-Value ($n = 72$)
		0 kGy	0.5 kGy	0.8 kGy	1 kGy		^{60}Cobalt	Electron-beam		
1	Isorhamnetin-hexosyl-pentosyl-hexoside	6.0 ± 0.1	5.9 ± 0.4	8.0 ± 1	6 ± 1	<0.001	7 ± 1	6 ± 1	<0.001	<0.001
2	Quercetin-3-*O*-(6-*O*-rhamnosylglucoside)-7-*O*-rhamnoside	46 ± 1	48 ± 5	53 ± 8	59 ± 10	<0.001	57 ± 9	46 ± 2	<0.001	<0.001
3	Isorhamnetin-3-*O*-(6-*O*-rhamnosyl-galactoside)	5.2 ± 0.1	4.4 ± 0.5	5.5 ± 0.5	6 ± 1	<0.001	6 ± 1	5 ± 1	<0.001	<0.001
4	Acetyl-quercetin-3-*O*-(6-*O*-rhamnosylglucoside)-7-*O*-rhamnoside	12.6 ± 0.4	14 ± 1	14 ± 1	11.5 ± 0.3	<0.001	13 ± 1	12 ± 1	0.015	<0.001
5	Kaempferol-3-*O*-(6-*O*-rhamnosylglucoside)-7-*O*-rhamnoside	3.0 ± 0.2	3.1 ± 0.3	3.6 ± 0.3	3.7 ± 0.5	<0.001	3.6 ± 0.5	3.1 ± 0.2	<0.001	<0.001
6	Violanthin (apigenin-6-*C*-glucosyl-8-*C*-rhamnoside)	2.1 ± 0.1	1.8 ± 0.1	2.1 ± 0.2	2.1 ± 0.2	<0.001	2.1 ± 0.3	1.9 ± 0.2	0.001	<0.001
7	Isorhamnetin-3-*O*-(2,6-di-*O*-rhamosyl-glucoside)	5.1 ± 0.2	5.6 ± 0.5	6 ± 1	6 ± 1	0.001	6 ± 1	5.0 ± 0.3	<0.001	<0.001
8	Quercetin-3-*O*-rutinoside	28 ± 1	29 ± 1	24 ± 1	30 ± 1	<0.001	28 ± 2	28 ± 3	0.398	<0.001
9	Kaempferol-3-*O*-rutinoside	2.5 ± 0.2	2.6 ± 0.5	2.7 ± 0.5	2.5 ± 0.1	0.587	2.9 ± 0.4	2.2 ± 0.2	<0.001	<0.001
10	Isorhamnetin-3-*O*-rutinoside	1.6 ± 0.1	1.5 ± 0.5	1.4 ± 0.3	1.3 ± 0.1	0.029	1.6 ± 0.3	1.3 ± 0.3	<0.001	<0.001
11	Cyanidin-3-*O*-rutinoside	0.70 ± 0.04	0.8 ± 0.2	0.7 ± 0.3	1.0 ± 0.2	0.004	1.0 ± 0.2	0.6 ± 0.2	<0.001	<0.001
12	Delphinidin-3-*O*-rutinoside	3.3 ± 0.2	13.3 ± 0.5	3 ± 1	4 ± 1	0.099	4 ± 1	2.8 ± 0.4	<0.001	<0.001
13	Delphinidin-3-(4″-*p*-coumaroyl)-rutinoside-5-glucoside	10.2 ± 0.5	10 ± 1	10 ± 3	11 ± 3	0.198	12 ± 2	8 ± 1	<0.001	<0.001
14	Cyanidin-3-(coumaroyl)-methylpentosyl-hexosyl-5-hexoside	6.7 ± 0.2	7 ± 1	5 ± 1	6 ± 1	<0.001	7 ± 1	5 ± 1	<0.001	<0.001

(di- or trisaccharide). Compound **10** was positively identified as isorhamnetin-3-*O*-rutinoside according to its retention time, mass and UV–Vis characteristics by comparison with a commercial standard. Compound **3** presented the same mass spectrum as compound **10**, but it elutes earlier. Some structural possibilities could be envisaged for that compound, such as containing a neohesperidose moiety [*i.e.*, isorhamnetin-3-*O*-(2-*O*-rhamosyl-glucoside)] or having a different hexosyl residue [*i.e.*, isorhamnetin-3-*O*-(6-*O*-rhamosyl-galactoside)]. Both compounds would be expected to elute earlier than isorhamnetin-3-*O*-rutinoside in reversed phase. Although the precise identity and position of the sugar substituents cannot be concluded from the LC–MS data, compound **3** was tentatively assigned as isorhamnetin-3-*O*-(6-*O*-rhamosyl-galactoside), considering the identification of this compound together with isorhamnetin-3-*O*-(6-*O*-rhamosyl-glucoside) (*i.e.*, isorhamnetin-3-*O*-rutinoside) in petals of *Catharanthus roseus* shown by Ferreres et al. (2008). In both cases elution and spectral characteristics were similar to the ones observed in our study. Mass spectra of compound **7** ($[M-H]^-$ at *m/z* 769) suggested the presence of one hexosyl and two deoxyhexosyl moieties attached to isorhamnetin. A compound with a similar UV spectrum, pseudomolecular ion and fragmentation pattern was tentatively identified in the seeds of *Catharanthus roseus* by Ferreres et al. (2008), as isorhamnetin-3-*O*-(2,6-di-*O*-rhamosyl-glucoside), so that this identity was tentatively assumed for the compound detected in our sample. The precise identity and position of the sugar substituents in compound **1** could not be established, and therefore it was tentatively identified as isorhamnetin-hexosyl-pentosyl-hexoside based on its pseudomolecular ion.

Compounds **2** ($[M-H]^-$ at *m/z* 755), **4** ($[M-H]^-$ at *m/z* 797) and **8** ($[M-H]^-$ at *m/z* 609) showed absorption and mass spectra coherent with quercetin-glycosides. Compound **8** was positively identified as quercetin-3-*O*-rutinoside according to its retention time, mass and UV–Vis characteristics by comparison with a commercial standard. The mass spectrum of compound **2** suggested a quercetin glycoside containing two deoxyhexoses and one hexose. Two structures with this substitution pattern have been previously reported in *Viola odorata* (quercetin-3-*O*-α-rhamnopyranosyl-(1 → 2)-[α-rhamnopyranosyl-(1 → 6)]-β-glucopyranoside; Karioti, Furlan, Vincieri, & Bilia, 2011) and *V. tricolor* (quercetin-3-*O*-deoxyhexosylhexoside-7-*O*-deoxyhexoside; Vukics, Ringer, et al., 2008). The mass fragmentation of the compound obtained in our study is coherent with the second structure; in particular the fragment at *m/z* 343 (explained from the $^{0,2}X$ cleavage of the sugar attached at position 3 of quercetin plus loss of the deoxyhexosyl residue at position 7) would not be produced from a quercetin-*O*-triglycoside structure as proposed by Karioti et al. (2011). Furthermore, this fragment supports a 1–6 linkage between the sugars in the deoxyhexosylhexoside moiety instead of 1–2. The other fragments could be explained by the losses of the deoxyhexosyl residue (*m/z* at 609) and deoxyhexose (*m/z* at 591) at position 7, $^{0,2}X$ cleavage of the sugar at position 3 (*m/z* 489) and the loss of all sugar residues (*m/z* at 301, quercetin). Although the nature of the sugar residues and their precise location on the aglycon could not be concluded from the available data, the positions C-3 and C-7 can be proposed, as they have been indicated as the preferred attachment points for *O*-glycosyl units (Cuyckens & Claeys, 2004) and due to the abundance of quercetin-3-*O*-rutinoside in the sample. All in all, compound **2** (Fig. 1A) was tentatively identified as quercetin-3-*O*-(6-*O*-rhamnosyl-glucoside)-7-*O*-rhamnoside. Compound **4** showed a molecular weight 42 mu higher than compound **2**, pointing to an acetylated form of the latter.

UV and mass spectra of compounds **5** and **9** might correspond to kaempferol derivatives. Compound **9** ($[M-H]^-$ at *m/z* 593) was positively identified as kaempferol-3-*O*-rutinoside by comparison of its chromatographic and spectral characteristics with a commercial standard. The pseudomolecular ion of compound **5** ($[M-H]^-$ at *m/z* 739) indicated a kaempferol glycoside bearing two deoxyhexoses and one hexose; although the nature and linkage position of the sugars could not be concluded from the available data, by analogy with the above discussed compound **2** it was tentatively assigned as kaempferol-3-*O*-(6-*O*-rhamnosyl-glucoside)-7-*O*-rhamnoside.

Compound **6** showed a pseudomolecular ion $[M-H]^-$ at *m/z* 577, releasing MS^2 fragment ions at *m/z* 517 ($[M-H-60]^-$), 487 ($[M-H-90]^-$), 473 ($[M-H-104]^-$), 457 ($[M-H-120]^-$), 383 (agl + 113) and 353 (agl + 83) that are characteristic of *C*-glycosylated flavones (Cuyckens & Claeys, 2004; Ferreres, Silva, Andrade, Seabra, & Ferreira, 2003). These features are in agreement with the structure of violanthin (apigenin-6-*C*-glucosyl-8-*C*-rhamnoside), a compound firstly identified in *V. tricolor* by Hörhammer et al. (1965) and that has been consistently reported in this (Wagner et al., 1972; Vukics, Kery, et al., 2008; Vukics, Ringer, et al., 2008) and in other *Viola* species (Carnat, Carnat, Fraisse, & Lamaison, 1998; Flamini, 2007).

Compounds **11**–**14** (Fig. 1B) were identified as anthocyanins derived from cyanidin and delphinidin, based on their absorption and mass spectra. Molecular ions of compounds **11** ($[M+H]^+$ at *m/z* 595) and **12** ($[M+H]^+$ at *m/z* 611) indicated the existence of deoxyhexosyl and hexosyl substituents. The observation of MS^2 fragments at *m/z* 449 and 465 from the loss of the deoxyhexosyl residue (−146 mu), and the absence of fragments from the loss of the hexosyl residue (162 mu) pointed that the two sugars constituted a disaccharide. This fragmentation pattern was consistent with that indicated by Giusti, Rodrıguez-Saona, Griffin, and Wrolstad (1999) for anthocyanin C3-rutinosides, according to which the linkage 1–6 between rhamnose and glucose (*i.e.*, rutinose) is more suited to fragmentation than the linkage 1–2 (*i.e.*, neohesperidose). Therefore, the compounds were tentatively identified as cyanidin 3-*O*-rutinoside (**11**) and delphinidin 3-*O*-rutinoside (**12**).

Molecular ions of compounds **13** ($[M+H]^+$ at *m/z* 919) and **14** ($[M+H]^+$ at *m/z* 903) matched the structures of the anthocyanins delphinidin-3-(4″-*p*-coumaroyl)-rutinoside-5-glucoside (violanin)

Table 3
Antioxidant activity of *Viola tricolor* extracts according to the irradiation dose and irradiation technology.

Assay	EC_{50} values (mg/ml of extract)								
	Irradiation dose (ID)				*p*-Value ($n = 18$)	Irradiation technology (IT)		*p*-Value ($n = 36$)	ID × IT *p*-Value ($n = 72$)
	0 kGy	0.5 kGy	0.8 kGy	1 kGy		^{60}Cobalt	Electron-beam		
DPPH radical-scavenging activity	0.25 ± 0.02	0.24 ± 0.02	0.26 ± 0.04	0.23 ± 0.02	<0.001	0.24 ± 0.03	0.25 ± 0.03	0.104	<0.001
Reducing power – Prussian blue assay	0.29 ± 0.01	0.20 ± 0.01	0.24 ± 0.04	0.32 ± 0.03	<0.001	0.27 ± 0.04	0.26 ± 0.05	0.505	<0.001
Reducing power – Folin–Ciocalteu assay*	177 ± 21	168 ± 11	188 ± 19	173 ± 10	0.004	176 ± 12	177 ± 21	0.866	<0.001
Inhibition of β-carotene bleaching	2.0 ± 0.3	1.6 ± 0.2	1.8 ± 0.2	1.5 ± 0.5	0.001	1.6 ± 0.4	1.9 ± 0.3	<0.001	<0.001

* Results expressed in mg of gallic acid equivalents (GAE) per g of extract.

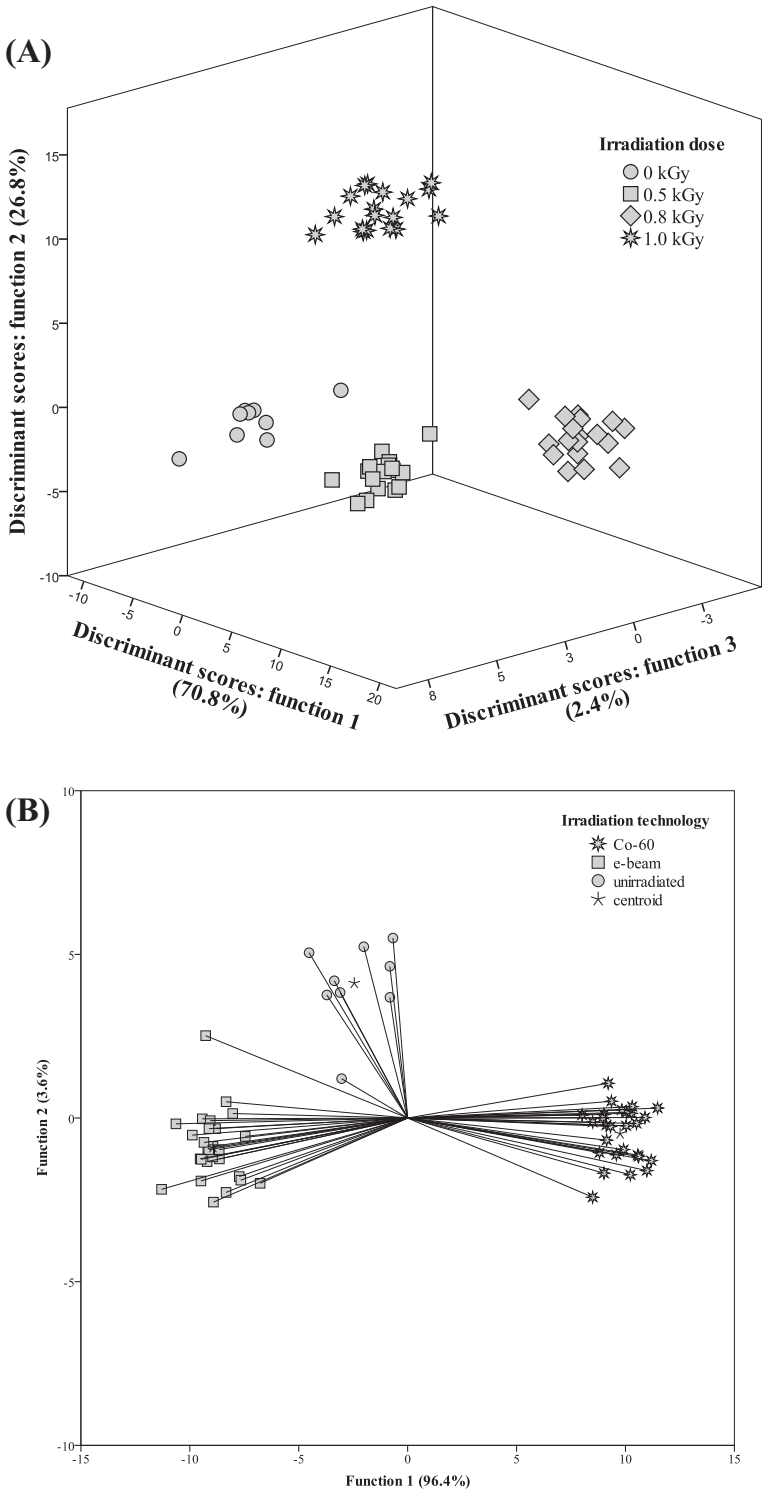

Fig. 2. Mean scores of different irradiation doses (A) or irradiation technology (B) projected for the discriminant functions defined from phenolic compounds profile and antioxidant activity assays results.

and cyanidin-3-(coumaroyl)-methylpentosyl-hexosyl-5-hexoside, tentatively identified by Karioti et al. (2011) in flowers of *V. odorata*. The presence of a shoulder around 310 nm is also coherent with the suggested identities, since this spectral characteristic is a strong indication for the existence of a *p*-coumaroyl residue. Therefore, compounds **13** and **14** were tentatively identified as the compounds mentioned above.

3.2. Effects of gamma and electron-beam irradiation on phenolic compounds and antioxidant activity

Besides characterizing the phenolic profile of *V. tricolor*, it was also intended to evaluate how this profile would be affected by gamma or electron-beam irradiations. Accordingly, the values presented in Table 2 refer to non-irradiated samples, as well as

to samples irradiated under different conditions. The values shown for each irradiation dose (ID) include results obtained for samples irradiated with ^{60}Co and electron-beam, in order to verify the best irradiation dose, independently of the used source. Likewise, values for each irradiation technology (IT) result from the average value of all the assayed doses, aiming to define the most suitable technology, regardless of ID. ID and IT were defined as statistical factors and their interaction, besides their individual contribution for the observed variance, was evaluated. As it can be concluded from Table 2, the interaction between factors was statistically significant ($p < 0.030$) in all cases, not allowing classification of each of them individually. Nevertheless, the effect of each factor was also significant in most cases, except for ID in compounds **9** ($p = 0.587$), **12** ($p = 0.099$) and **13** ($p = 0.198$) and for IT in compound **8** ($p = 0.398$). As depicted from the estimated marginal means (data not shown) produced in the GLM, all phenolic compounds (except compound **8**, which did not reveal significant differences) were detected in higher amounts in the gamma-irradiated samples, independently of the used dose. This occurrence might be due to differences in the atmospheric composition inside the polyethylene bags, where samples were kept, or to alterations in the molecular oxygen availability induced by the ionizing effect of gamma-irradiation. Regarding the effect of ID, the 1 kGy dose seemed to be advantageous (independently of the source) to obtain higher amounts of phenolic compounds. In fact, eight (**2**, **3**, **5**–**8**, **11** and **14**) out of the eleven compounds with statistical differences were quantified in higher amounts for this dose. Only compounds **6**, **10** and **14** were present in higher values in the non-irradiated samples.

Quercetin-3-*O*-(6-*O*-rhamnosylglucoside)-7-*O*-rhamnoside (compound **2**) was the most abundant compound in all the samples, representing more than 40% of the total phenolic compounds. In fact, the second (compound **8**) and third (compound **4**) most abundant compounds were also quercetin derivatives, indicating that *V. tricolor* might be considered a source of these phenolic compounds (Havsteen, 2002).

Among anthocyanins, delphinidin-3-(4″-*p*-coumaroyl)-rutinoside-5-glucoside was the one detected in the highest quantity, followed by the cyanidin derivative with the same glycosylation pattern. In view of the different phenotypes included in the sampling, a more complex anthocyanins profile could have been expected, but the results seem to indicate that *V. tricolor* is characterized by a restricted number of these compounds, independent of phenotype.

As it could have been anticipated from the differences in phenolic compounds quantity observed among the assayed ID or IT, the antioxidant activity was higher in the irradiated samples (Table 3). Samples irradiated with 1 kGy (independently of IT) showed the highest capacity to scavenge DPPH and inhibit β-carotene bleaching, while the strongest reducing power was observed in samples irradiated with 0.8 kGy (Folin–Ciocalteu assay) and 0.5 kGy (Prussian blue assay). Concerning the effect of IT, only β-carotene bleaching inhibition was significantly different for gamma and electron-beam irradiated samples, while the interaction among factors was again significant in all cases.

3.3. Linear discriminant analysis

Until this point, the effect of each factor (ID and IT) was evaluated by analyzing individual changes in each phenolic compound or antioxidant activity assay. Nevertheless, it is useful to perform a comprehensive study of the effect of each factor in all the studied parameters simultaneously. Accordingly, two linear discriminant analyses (LDA) (one for each factor) were performed to evaluate the global effects on the antioxidant activity and phenolic compounds profile. The significant independent variables (EC_{50} values for antioxidant activity assays and phenolic compounds content) were selected using the stepwise method of the LDA, according to the Wilks' λ test. All the variables were included in each analysis, but only variables with a statistically significant classification performance ($p < 0.05$) were selected by the software.

Considering the ID effect, 3 significant functions were defined (Fig. 2A), which included 100.0% of the observed variance (first, 70.8%; second, 26.8%; third, 2.4%). As it can be observed, the markers corresponding to the tested groups (0.0 kGy, 0.5 kGy, 0.8 kGy and 1 kGy) were distributed separately. The antioxidant activity among these samples was not strongly affected, since DPPH scavenging activity, β-carotene bleaching inhibition and reducing power (Folin–Ciocalteu assay) were not included by the model. Likewise, compounds **5**, **9**, **10**, **12** and **13** were also removed by the software. Function 1 (Fig. 2A) separated only markers corresponding to 0.8 kGy, indicating that compounds **1** (higher), **7**, **8**, **11** and **14**, which presented the highest correlations with function 1 (Table 4), underwent the highest changes when submitted to this ID. Function 2 was effective enough to separate non-irradiated samples from those irradiated with 0.5 kGy and 1 kGy, mainly to the differences observed for compounds **2** and **14**. The separation of these samples was improved with function 3, especially due to the contribution of compounds **2**, **7** and **14**. In terms of

Table 4
Canonical discriminant functions coefficients obtained to each variable selected when analyzing the ID and IT effects.

Variable	Function 1	Function 2	Function 3
ID effect			
1 – Isorhamnetin-hexosyl-pentosyl-hexoside	2.712	−0.738	−0.160
2 – Quercetin-3-*O*-(6-*O*-rhamnosylglucoside)-7-*O*-rhamnoside	0.573	2.487	−1.611
3 – Isorhamnetin-3-*O*-(6-*O*-rhamosyl-galactoside)	0.455	0.818	0.433
4 – Acetyl-quercetin-3-*O*-(6-*O*-rhamnosylglucoside)-7-*O*-rhamnoside	1.144	−0.531	−0.089
6 – Violanthin	0.341	−0.408	0.896
7 – Isorhamnetin-3-*O*-(2,6-di-*O*-rhamosyl-glucoside)	−2.177	0.436	−1.022
8 – Quercetin-3-*O*-rutinoside	−1.751	−0.087	−0.577
11 – Cyanidin-3-*O*-rutinoside	2.397	0.232	−0.877
14 – Cyanidin-3-(coumaroyl)-methylpentosyl-hexosyl-5-hexoside	−3.905	−2.752	2.664
Reducing power (Prussian Blue assay)	0.214	1.463	0.661
IT effect			
2 – Quercetin-3-*O*-(6-*O*-rhamnosylglucoside)-7-*O*-rhamnoside	1.045	−1.791	
4 – Acetyl-quercetin-3-*O*-(6-*O*-rhamnosylglucoside)-7-*O*-rhamnoside	0.452	−0.814	
6 – Violanthin	−0.037	0.858	
11 – Cyanidin-3-*O*-rutinoside	1.453	0.712	
13 – Delphinidin-3-(4″-*p*-coumaroyl)-rutinoside-5-glucoside	0.729	−0.540	
Reducing power (Prussian Blue assay)	−1.830	0.230	
Reducing power (Folin–Ciocalteu assay)	0.932	0.496	

classification performance, all the samples were correctly classified, both for original grouped cases, and for cross-validated grouped cases.

In the analysis carried out to evaluate the effect of IT, the discriminant model selected 2 significant functions (Fig. 2B), which also included 100.0% of the observed variance (function 1: 96.4%, function 2: 3.6%). The tested groups (non-irradiated, electron-beam and Co-60) were completely individualized, based on the selected variables: compounds **2**, **4**, **6**, **11** and **13** and both reducing power assays. Function 1 separated mainly samples irradiated with gamma-irradiation from those submitted to electron-beam irradiation, particularly (Table 2) as a result from differences observed among compounds **10** and **13** and also in the reducing power (Prussian blue assay). Function 2 was useful to separate non-irradiated samples (Fig. 2B), with compound **2** as the most effective variable. The classification performance was also completely correct for original grouped cases and for cross-validated grouped cases.

4. Conclusion

In general, gamma-irradiated samples gave higher amounts of phenolic compounds (except compound **8**, which did not reveal significant differences), independently of the applied dose. Moreover, these compounds were favored by 1 kGy dose, either using Co-60 or electron-beam. The three most abundant compounds (compounds **2**, **4** and **8**) were quercetin glycosides, which showed significant variation within different doses or technologies.

The antioxidant activity was also higher in the irradiated samples, especially those treated with 1 kGy (independently of IT), which showed the highest capacity to scavenge DPPH and to inhibit β-carotene bleaching. On the other hand, the IT had no significant effects on the antioxidant activity, except for β-carotene bleaching inhibition (higher in gamma-irradiated samples).

The LDA outcomes indicated that differences among the phenolic compounds, or antioxidant activity, effectively discriminate between the assayed doses and the technologies, showing also which variables contributed most. This information might be useful to define which dose and/or technology optimizes the content of a specific phenolic compound.

Overall, irradiation did not negatively affect the levels of phenolic compounds and antioxidant activity, offering the possibility of its application to expand the shelf life of *V. tricolor* and highlighting new commercial solutions for this functional food.

Acknowledgments

The authors are grateful to the Fundação para a Ciência e a Tecnologia (FCT, Portugal) for financial support to CIMO (strategic project PEst-OE/AGR/UI0690/2011), João C.M. Barreira (SFRH/BPD/72802/2010 grant) and L. Barros (“Compromisso para a Ciência 2008” contract). The GIP-USAL is financially supported by the Spanish Government through the *Consolider-Ingenio 2010* Programme (FUN-C-FOOD, CSD2007-00063). To CNEN, CAPES, CNPq and IPEN-CNEN/SP for financial support to Amanda Koike. This research is included in a Bilateral action FCT-CNPq, Portugal/Brazil 2014.

References

Anderson, R., Schnelle, R., & Bastin, S. (2012). *Edible flowers* – University of Kentucky – College of Agriculture, Food and Environment. Retrieved from <http://www.uky.edu/Ag/CDBREC/introsheets/edible.pdf> [02.07.2014].

Carnat, A.-P., Carnat, A., Fraisse, D., & Lamaison, J.-L. (1998). Violarvensin, a new flavone di-C-glycoside from *Viola arvensis*. *Journal of Natural Products, 61*, 272–274.

Creasy, R. (1999). *The edible flowers garden*. Boston: Periplus Editions.

Cuyckens, F., & Claeys, M. (2004). Mass spectrometry in the structural analysis of flavonoids. *Journal of Mass Spectrometry, 39*, 1–15.

Fan, X., Niemira, B. A., & Sokorai, K. J. B. (2003). Sensorial, nutritional and microbiological quality of fresh coriander leaves as influenced by ionizing radiation and storage. *Food Research International, 36*, 713–719.

Farkas, J. (2006). Irradiation for better foods. *Trends in Food Science & Technology, 18*, 1–5.

Farkas, J., & Mohácsi-Farkas, C. (2011). History and future of food irradiation. *Trends in Food Science & Technology, 20*, 1–6.

Ferreres, F., Pereira, D. M., Valentão, P., Andrade, P. B., Seabra, R. M., & Sottomayor, M. (2008). New phenolic compounds and antioxidant potential of *Catharanthus roseus*. *Journal of Agricultural and Food Chemistry, 56*, 9967–9974.

Ferreres, F., Silva, B. M., Andrade, P. B., Seabra, R. M., & Ferreira, M. A. (2003). Approach to the study of *C*-glycosyl flavones by ion trap HPLC–PAD–ESI/MS/MS: Application to seeds of quince (*Cydonia oblonga*). *Phytochemistry Analysis, 14*, 352–359.

Flamini, G. (2007). Flavonoids and other compounds from the aerial parts of *Viola etrusca*. *Chemistry & Biodiversity, 4*, 139–144.

García-Marino, M., Hernández-Hierro, J. M., Rivas-Gonzalo, J. C., & Escribano-Bailón, M. T. (2010). Colour and pigment composition of red wines obtained from comaceration of *Tempranillo* and *Graciano* varieties. *Analytical Chimica Acta, 660*, 134–142.

Giusti, M. M., Rodrıguez-Saona, L. E., Griffin, D., & Wrolstad, R. E. (1999). Electrospray and tandem mass spectroscopy as tools for anthocyanin characterization. *Journal of Agricultural and Food Chemistry, 47*, 4657–4664.

Gonçalves, A. F. K., Friedrich, R. B., Boligon, A. A., Piana, M., Beck, R. C. R., & Athayde, M. L. (2012). Anti-oxidant capacity, total phenolic contents and HPLC determination of rutin in *Viola tricolor* (L) flowers. *Free Radicals and Antioxidants, 2*, 32–37.

Havsteen, B. H. (2002). The biochemistry and medical significance of the flavonoids. *Pharmacology & Therapeutics, 96*, 67–202.

Hellinger, R., Koehbach, J., Fedchuk, H., Sauer, B., Huber, R., Gruber, C. W., & Gründemann, C. (2014). Immunosuppressive activity of an aqueous *Viola tricolor* herbal extract. *Journal of Ethnopharmacology, 151*, 299–306.

Hörhammer, L., Wagner, H., Rosprim, L., Mabry, T., & Rösler, H. (1965). Über die struktur neuer und bekannter flavon-C-glycoside. *Tetrahedron Letters, 22*, 1707–1711.

Jauron, R., Beiwel, J., & Naeve, L. (2013) *Edible flowers* – Iowa State University – Extension and Outreach. Retrieved from <https://store.extension.iastate.edu/Product/rg302-pdf> [02.07.2014].

Karioti, A., Furlan, C., Vincieri, F. F., & Bilia, A. R. (2011). Analysis of the constituents and quality control of *Viola odorata* aqueous preparations by HPLC–DAD and HPLC–ESI-MS. *Analytical and Bioanalytical Chemistry, 399*, 1715–1723.

Kelley, K. M., Cameron, A. C., Biernbaum, J. A., & Poff, K. L. (2003). Effect of storage temperature on the quality of edible flowers. *Postharvest Biology and Technology, 27*, 341–344.

Komolprasert, V. (Ed.). (2007). *Packaging for foods treated by ionizing radiation* & Han, Jung H. (Eds.). *Packaging for nonthermal processing of food* (pp. 87–116). IFT Press: Blackwell Publishing.

Mabry, T. J., Markham, K. R., & Thomas, M. B. (1970). *The systematic identification of flavonoids*. New York: Springer. 354 pp.

Mlcek, J., & Rop, O. (2011). Fresh edible flowers of ornamental plants – A new source of nutraceutical foods – A review. *Trends in Food Science & Technology, 22*, 561–569.

Morehouse, K. M. (2002). Food irradiation – US regulatory considerations. *Radiation Physics and Chemistry, 63*, 281–284.

Newman, S. E., & O'Conner, A. S. (2009). *Edible Flowers. CSU Extension, 7237*, 1–5.

Piana, M., Silva, M. A., Trevisan, G., de Brum, T. F., Silva, C. R., Boligon, A. A., et al. (2013). Antiinflammatory effects of *Viola tricolor* gel in a model of sunburn in rats and the gel stability study. *Journal of Ethnopharmacology, 150*, 458–465.

Vukics, V., Kery, A., Bonn, G. K., & Guttman, A. (2008a). Major flavonoid components of heartsease (*Viola tricolor* L.) and their antioxidant activities. *Analytical and Bioanalytical Chemistry, 390*, 1917–1925.

Vukics, V., Ringer, T., Kery, A., Bonn, G. K., & Guttman, A. (2008b). Analysis of heartsease (*Viola tricolor* L.) flavonoid glycosides by micro-liquid chromatography coupled to multistage mass spectrometry. *Journal of Chromatography A, 1206*, 11–20.

Wagner, H., Rosprim, L., & Düll, P. (1972). The flavone-C-glycosides of *Viola tricolor* L. *Zeitschrift für Naturforschung B, 27*, 954–958.